Phenotyping characterization of methylmercury marine bacteria detoxifiers

Autor: Miguel Capilla Lloris,
Supervisors: Olga Sanchez[1] and Silvia González Acinas[2]

[1] Departament de Genètica i Microbiologia, Facultat de Biociències, Universitat Autònoma de Barcelona, E-08193 Bellaterra, Spain [2]Departament de Biologia Marina i Oceanografia, Institut de Ciències del Mar, ICM-CSIC, E-08003 Barcelona, Spain

Abstract

Mercury (Hg) is a toxic heavy metal with an even more toxic form, methylmercury (MeHg). MeHg is a neurotoxic compound that can reach human population through consumption of big fish. It is mainly formed in the sediments by anaerobic bacteria in aquatic depths. However, bacteria have developed resistance mechanisms against this toxic, by harbouring the *mer* operon, which gives them the capacity to volatilize this MeHg. Some marine bacteria, like *Alteromonas* and *Marinobacter* spp., include the *mer* operon and therefore have the potential to remove this pollutant from the environment. In this study, the growth characteristics from marine isolates belonging to *Alteromonas* and *Marinobacter* were stablished at different MeHg concentrations (0, 1, 2.5 and 5 µM) measuring optical density (OD_{600}). *Alteromonas* was able to grow at 5 µM, displaying a higher resistance to MeHg than *Marinobacter* that was only capable of growing at 1 µM of MeHg. Additionally, epifluorescence microscopy for cell counting and inclusion bodies (IBs) quantification was performed. Also scanning transmission electron microscopy (STEM)-Energy Dispersive X-Ray Microscopy (EDX) was used to examine the nature of those IBs at the highest resolution. The results confirmed that *Alteromonas* produced higher number of IBs inside their cells associated with Polyphosphate (poly-P). In summary, due to its tolerance for growing in MeHg, *Alteromonas* is a clear candidate to be used in bioremediation of MeHg in marine environments.

Introduction

In nature, microorganisms interact with minerals and metals from the ecosystems changing their physico-chemical properties so they can get profit for their growth, activity and survival but also benefit other microorganisms in the ecosystem [Gadd *et al*. 2010]. Bacteria not only participate but also display ecologically relevant roles in all the biogeochemical cycles in the planet including Hg.

Hg is the most toxic heavy metal that can be found due to its high affinity to the sulfhydryl residues of the lateral chains of aminoacids [Nies, 2003]. Besides of being toxic, Hg is very dangerous because it can be found worldwide and can be transformed into a more toxic form as it is MeHg. Hg can come from natural sources (ie volcanic activity, burnt of vegetation, etc) or anthropogenic sources (ie. use of carbon, mining, etc) although most of the Hg that can be found nowadays comes from anthropogenic sources starting in the Industrial Revolution (18^{th} century) until reaching a maximum peak in the seventies of the last century when its production began to reduce [UNEP Chemicals Branch, 2008].

MeHg is a neurotoxic compound that reach to humans through consumption of food, such as big fish (like tuna), that previously have been in contact with MeHg and bioaccumulated through the marine food web. MeHg can affect pregnant woman since it can cross the placenta and cause anomalies in the fetus [Kim and Zoh, 2012]. This MeHg is mostly formed in the sediments from the aquatics depths due to the activity of anaerobic bacteria [Figure 1; Boyd *et al*. 2012].

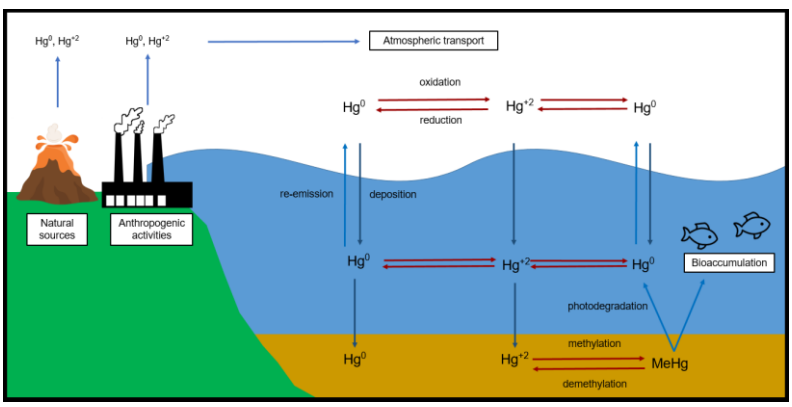

Figure 1. Biochemical cycle of Hg and MeHg. Briefing of the Hg cycle where we found three dominant species (Hg^0, Hg^{+2} and MeHg). Hg^0 and Hg^{+2} are released to the atmosphere where they can be taken by the water masses and set in the sediments or transformed into MeHg, bioaccumulate in the marine organisms and at the end being assimilated by humans through consumption. Font: Modified from Kim & Zoh (2012).

Some aerobic bacteria and archaea have developed resistance mechanisms against Hg species. This resistance is mainly encoded in the *mer* operon, although other resistance mechanisms can be found, as biosorption or precipitation by exopolysaccarides (EPS) [François *et al*. 2011] or bioaccumulation [Hoque & Fritscher 2016]. The *mer* operon encode for several proteins, not necessarily found all of them in the same organism. The most important is MerA, the Hg reductase enzyme which takes care of the transformation of the Hg species. There are also MerB, an organomercurial lyase, an enzyme that cleaves the carbon-mercury bond releasing methane [Schottel 1978]; MerP, a periplasmic Hg^{+2} scavenging protein; MerT, MerC, MerE, MerF and MerG , which act as inner-membrane spanning proteins and one or two regulatory proteins, MerR and MerD. In order to degrade MeHg, this is transported by MerE inside the cell, where MerB carries out the removal of the methyl group and MerA reduces mercury to Hg^0, which diffuses out of the cell [Boyd *et al*. 2012 and Lin *et al*. 2012].

The problem of MeHg on public health is of big concern and therefore it is crucial to isolate and characterize marine bacteria with the capacity to remove this compound from contaminated marine ecosystems. Thus, the aim of this study is (i) to advance in the mechanisms of how marine bacteria strains related to *Alteromonas* and *Marinobacter* spp. remove MeHg from the environment and (ii) to characterize their growth and physiological characteristics in the presence of this pollutant.

Material and methods

Microorganisms. Two strains previously isolated from the Atlantic Ocean (2000 m deep) from *Malaspina* Global Expedition were tested: *Alteromonas sp.* (ISS 312) and *Marinobacter sp.* (ISS 348).

Growth curves. Growth curves of both strains were performed with Zobell Marine Broth (medium composition per 1L: 1g yeast extract, 5g peptone, 750 mL filtered marine water and 250 mL MQ-water) and with 0, 1, 2.5 and 5 µM final concentration from a stock solution (50 µM) of MeHg (II) chloride (Alfa Aesar, Thermo Fisher Scientific, Germany). In each experiment, a killed cells control and a negative control without cells but with MeHg were also included. Growth curves were carried out in triplicate for each concentration. Samples were taken in order to determine (i) the optical density (OD_{600}) with a Varian Cary 100 Bio Spectrophotemeter (Agilent Technologies, USA), and (ii) the concentration of cells through DAPI staining.

Cell counts and quantification of inclusions bodies (IBs). Samples were fixed with glutaraldehyde, final volume 10% v/v, for at least two hours at 4ºC. Fifty µl of the sample diluted with 5 ml of 0.2 µm filtered MQ-water was stained with 50 µl DAPI (0.5 mg/ml) in the dark for 5 minutes and then filtrated through a polycarbonate black 25 mm 0.2 µm membrane disk (GVS Life Sciences, USA). Images from the filters were acquired using an Axio Imager.Z2m epifluorescence microscope connected to a Zeiss camera (AxioCam MRm, Carl Zeiss MicroImaging, S.L., Barcelona, Spain) at 630× magnification through the Axiovision software, and analyzed using ACMEtool2 [http://www.technobiology.ch/index.php?id=acmetool].

STEM (Scanning Transmission Electron Microscopy) – EDX (Energy Dispersive X-Ray Microscopy). Samples from the stationary phase of each growth curve were collected and fixed following the protocol of Moussa *et al.* (2007), changing the fixator (2% paraformaldehyde, 2.5% glutaraldehyde) and for dehydration, staining and microtomy Lee *at al.* (2008) was followed in the Servei de Microscopia from UAB. For final processing STEM-EDX analysis was made with an FEI Tecnai G2 F20 S-TWIN HR(S)TEM (Thermo Fisher Scientific, USA) working at 200kV from the Catalan Institute of Nanoscience and Nanotechnology (ICN2).

Results

Growth curves of *Alteromonas sp*. and *Marinobacter sp*. growing at different concentrations of MeHg are represented in Figure 2A and 2B. No growth was observed in the case of *Marinobacter* sp. at 2.5 and 5 µM. Table 1 shows the maximum growth rates for each culture and concentration of MeHg, where higher concentrations of MeHg resulted in a reduction of the maximum growth rate.

A comparison between 4,6-diamidino-2-phenylindole (DAPI) staining and STEM from *Alteromonas* and *Marinobacter* in their stationary phase (48 hours for *Alteromonas* and 72 hours for *Marinobacter*) is shown in Figure 3.

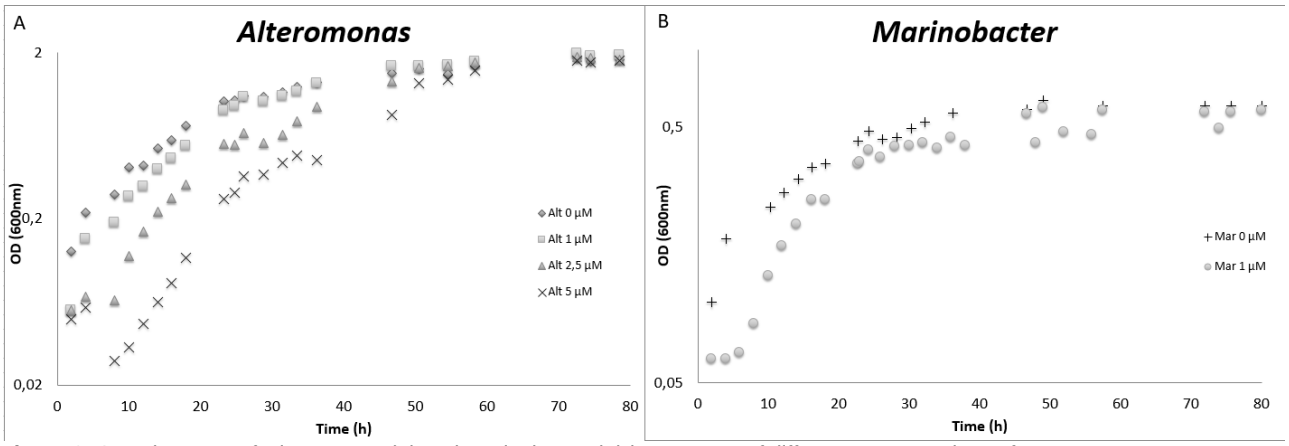

Figure 2. Growth curves of *Alteromonas* (A) and *Marinobacter* (B) in presence of different concentrations of MeHg.

Table 1. Maximum growth rate of *Alteromonas* sp. and *Marinobacter* sp. ND: no data.

Sample	*Alteromonas sp.*	*Marinobacter sp.*
0 µM	0.088 h^{-1}	0.067 h^{-1}
1 µM	0.088 h^{-1}	0.069 h^{-1}
2.5 µM	0.069 h^{-1}	ND
5 µM	0.052 h^{-1}	ND

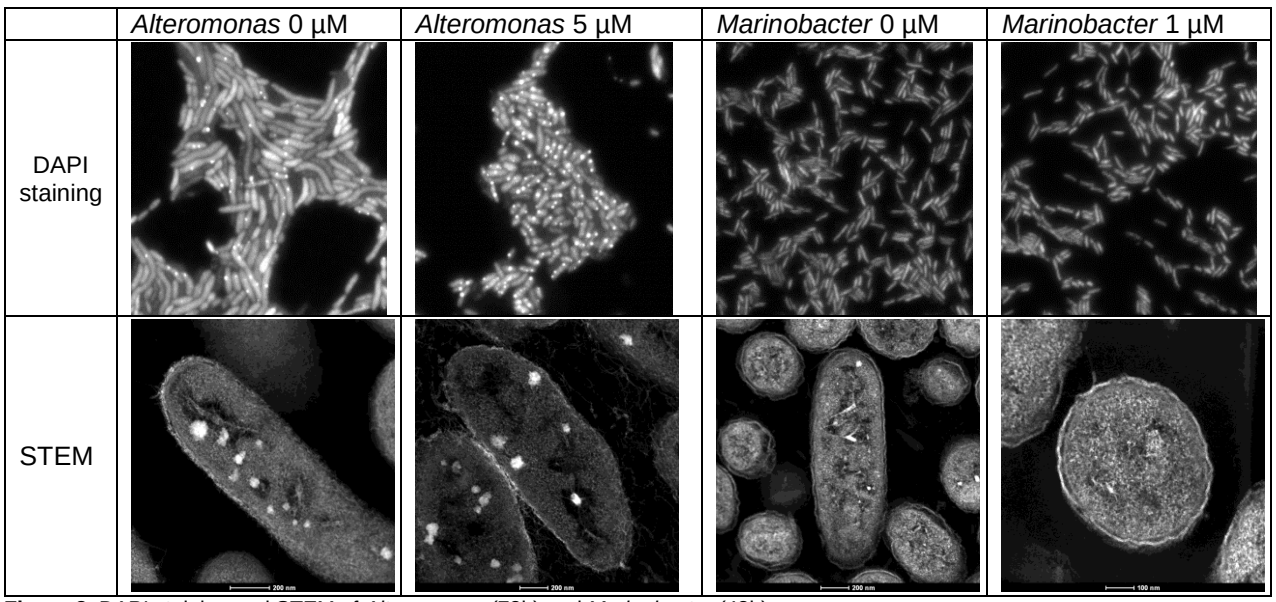

Figure 3. DAPI staining and STEM of *Alteromonas* (72h) and *Marinobacter* (48h).

As seen in Figure 3, only *Alteromonas* produced inclusion bodies (IBs). *Alteromonas* produced IBs during its exponential growth at 0, 1 and 2.5 µM and they started to disappear rapidly as the stationary phase developed and nutrient starvation began, while at 5 µM the highest number of IBs were detected reaching the stationary phase probably due to lower growth observed at this concentration (see yellow labels in Table 2). In Figure S1, a comparison of all concentrations at their highest IBs percentage.

Table 2. *Alteromonas'* cell density (cells/ml) and percentage of cells with IBs calculated with ACMEtool2. ND: no data. Numbers marked with a yellow shadow indicate those times where the % of IBs was maximal in each concentration.

	0 µM		1 µM		2.5 µM		5 µM	
Time	**cells/ml**	**% IB**	**cells/ml**	**% IB**	**cells/ml**	**% IB**	**cells/ml**	**% IB**
2	1,86E+07	ND	1,72E+07	ND	1,69E+07	16,40	1,31E+07	ND
6	5,40E+07	ND	2,98E+07	31,29	1,96E+07	32,86	1,50E+07	ND
12	9,76E+07	23,09	5,80E+07	34,73	3,53E+07	36,65	2,96E+07	17,20
16	1,23E+08	40,55	7,42E+07	32,28	5,22E+07	50,59	3,42E+07	19,45
24	2,31E+08	55,91	2,12E+08	61,77	7,80E+07	57,50	6,24E+07	36,33
28	3,83E+08	66,42	3,43E+08	71,20	1,55E+08	56,50	8,67E+07	43,75
36	4,47E+08	72,28	3,23E+08	80,21	3,20E+08	63,47	1,19E+08	56,12
48	5,33E+08	14,24	6,66E+08	23,73	6,68E+08	39,51	2,52E+08	59,20
54	5,08E+08	16,60	8,69E+08	10,22	8,70E+08	16,98	6,15E+08	64,29
72	5,57E+08	ND	9,45E+08	ND	7,77E+08	18,94	7,08E+08	ND

EDX analysis was carried out during the imaging procedure with the electron microscope to accomplish the elemental composition of IBs in *Alteromonas* sp. as is shown in Figure 4 (A, B and C). Different elements such as carbon, oxygen and phosphorus were measured in different sections of the cell (membrane, cytoplasmic and IB) for the control (0 µM) and at 5 µM of MeHg, but only IBs data are shown. Our results indicated that the carbon content was reduced when cells grew at 5 µM, while oxygen remained constant and phosphorus increased when Alteromonas grew with MeHg. However, elemental composition data tended to be more disperse in MeHg IBs (Figure 4A and 4C, black arrows). On the other hand, according to the work of Toso et al. (2011), the oxygen vs phosphorus elemental ratio may indicate the possible nature of the IBs (Figure 4D), being approximately 4.4 in the control and 3.3 in MeHg, which pointed to polyphosphate (poly-P) as the nature of such IBs.

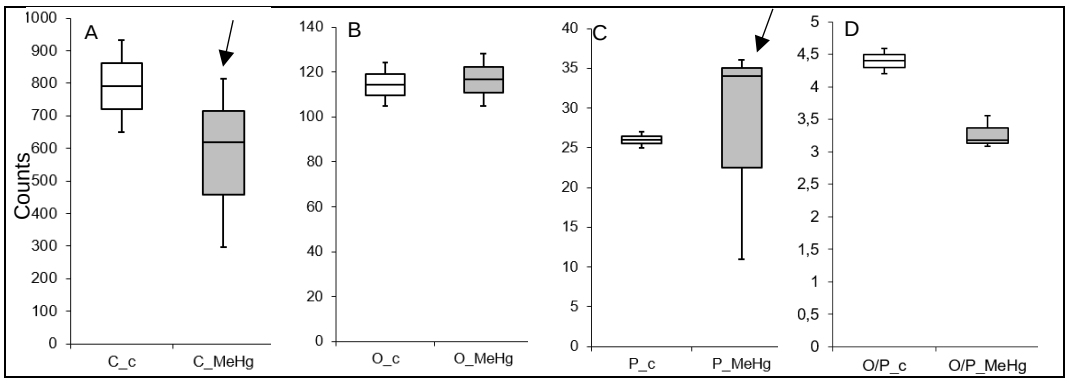

Figure 4. Box-plot representation of the elemental composition from IBs of *Alteromonas* sp. for the control at 0 µM of MeHg (c) and at 5 µM of MeHg (MeHg). **A**, carbon (C); **B**, oxygen (O), **C** phosphorus (P) and **D**, O/P ratio intensity peak. Black arrows indicate those data where main differences between control and MeHg was found and with higher dispersion in MeHg.

Discussion

The tested strains of *Alteromonas* and *Marinobacter* spp. showed MeHg resistance, being able to grow at several concentrations of this pollutant due to the fact that both of them have the *merAB* genes that detoxify MeHg to Hg^0. However, *Alteromonas* displayed higher resistance since it was capable of growing at 5 µM of MeHg, while *Marinobacter* was unable to grow at 2.5 and 5 µM of MeHg. In view of these results we decided to focus on *Alteromonas* in future experiments as it seems a more suitable candidate for bioremediation purposes.

The *Alteromonas* sp. exponential phase started right after MeHg was removed from the culture (approximately 6 hours after the addition of the inoculum at 1µM and 24 h later at 5 µM of MeHg), implying the need for the removal of most of the toxic first in order to start growing (data not shown).

Although some *Alteromonas* spp. can biosorpt metal ions, like Cr, Ni or Cu, by the production of EPS [Zhang Z. *et al*. 2017] no trace of Hg was found in the STEM-EDX analysis from the EPS or any other part of the cell (data not shown). This would mean that MeHg volatilized as expected by the action of the *mer* operon.

The nature of the IBs can vary from bacteria to bacteria, being these structures mainly constituted by poly-P, polyhydroxialcanoates (PHA) or proteins [Jiang X. *et al*. 2015]. In view of the results presented, IBs were always present in *Alteromonas* but they were more common in the exponential phase with more than 60% of the cells having at least one inclusion inside. This percentage started to reduce as the media exhausted, indicating that *Alteromonas* IBs may be used as an energy storage system, as are poly-P inclusions [Achbergerová and Nahálka 2011].

Elemental composition analyzed by means of EDX indicated less C, more P and similar O in the presence of MeHg compared to the control without MeHg, while the ratios O/P showed increase of P in IBs when growing in toxic conditions (Figure 3). Studies from Toso *et al*. (2011) demonstrated that inclusions with a ratio O/P between 5 to 3 were formed by poly-P inclusions. In fact, the theoretical O/P ratio should be closer to 3:1, as poly-P forms long chains of poly-anionic phosphate in the form of $(CatPO_3)_n$ (Cat would be a monovalent cation and n the length of the polymer chain); however the ratio depends on the length of the chain and on the presence of other oxygen atoms that are close to the granules and can contribute to this ratio. In our study, the *Alteromonas* O/P ratio was close to 3 (mean of 3.3) when the microorganism grew in the presence of MeHg, and higher in the control (mean of 4.4), probably due to phosphorus consumption resulting in an increase of the ratio (Figure 4D). In view of these data, supported by the images from DAPI-stained inclusions (poly-P can be stained with DAPI [Tijssen J. *et al*. 1982]) it can be concluded that the IBs from *Alteromonas* are poly-P inclusions.

Nonetheless, further experiments should be carried out to quantify the number of IBs along time in the growth curve of *Alteromonas* sp. with STEM-EDX, as well as to explore the expression of *merAB* genes in this process.

Acknowledgments

I thank Silvia Gonzalez and Olga Sanchez for taking me as a student and for their advices. Isa Sanz for teaching me and Raquel Ledo for her help. Also, Carla Pereira, Eli Sà and the other people from ICM, specially Irene Forn and Marta Sebastián, as well as Nuria Vigués and all the people from UAB.

Bibliography

Accardi A, Miller C. 2004. Secondary active transport mediated by a prokaryotic homologue of ClC Cl- channels. Nature **427**:803–807. **Achbergerová L, Nahálka J**. 2011. Polyphosphate - an ancient energy source and active metabolic regulator. Microb Cell Fact **10**:63.

Boyd ES, Barkay T. 2012. The mercury resistance operon: From an origin in a geothermal environment to an efficient detoxification machine. Front Microbiol **3**:1–13.

François F, Lombard C, Guigner JM, Soreau P, Brian-Jaisson F, Martino G, Vandervennet M, Garcia D, Molinier AL, Pignol D, Peduzzi J, Zirah S, Rebuffat S. 2012. Isolation and characterization of environmental bacteria capable of extracellular biosorption of mercury. Appl Environ Microbiol **78**:1097–1106.

Hoque E, Fritscher J. 2016. A new mercury-accumulating *Mucor hiemalis* strain EH8 from cold sulfidic spring water biofilms. Microbiologyopen **5**:763–781.

Jiang XR, Wang H, Shen R, Chen GQ. 2015. Engineering the bacterial shapes for enhanced inclusion bodies accumulation. Metab Eng **29**:227–237.

Kim MK, Zoh KD. 2012. Fate and transport of mercury in environmental media and human exposure. J Prev Med Public Heal **45**:335–343.

Lin C-C, Yee N, Barkay T. 2012. Microbial transformations in the mercury cycle. Environ Chem Toxicol Mercur. **Chapter 5:**155–192.

Moussa, M., Perrier-Cornet, J.-M. & Gervais, P. 2007. Damage in Escherichia coli Cells Treated with a Combination of High Hydrostatic Pressure and Subzero Temperature. Appl. Environ. Microbiol. **73:** 6508–6518.

Nies DH. 2003. Efflux-mediated heavy metal resistance in prokaryotes. FEMS Microbiol Rev **27**:313–339.

Tijssen JPF, Beekes HW, Van Steveninck J. 1982. Localization of polyphosphates in *Saccharomyces fragilis*, as revealed by 4′,6-diamidino-2-phenylindole fluorescence. Biochim Biophys Acta - Mol Cell Res **721**:394–398.

Toso DB, Henstra AM, Gunsalus RP, Zhou ZH. 2011. Structural, mass and elemental analyses of storage granules in methanogenic archaeal cells. Environ Microbiol **13**:2587–99.

UNEP Chemicals Branch. 2008. The global atmospheric mercury assessment: sources, emissions and transport. UNEP-Chemicals, Geneva 44.

Zhang Z, Cai R, Zhang W, Fu Y, Jiao N. 2017. A Novel Exopolysaccharide with Metal Adsorption Capacity Produced by a Marine Bacterium *Alteromonas sp*. JL2810. Mar Drugs **15(6**): 175.

Annex

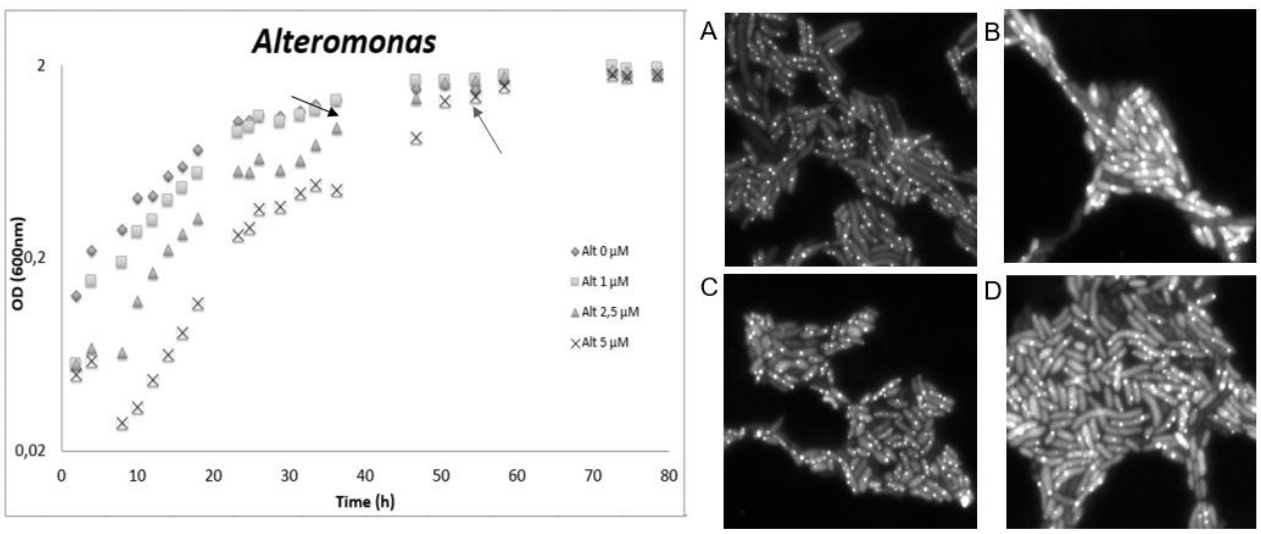

Figure S1. *Alteromonas'* growth curve growing at different concentrations of MeHg and epifluorescence microscope images of the cultures showing the maximum % IBs at different concentrations of MeHg. A, 0 µM; B, 1 µM; C, 2.5 µM (36h, black arrow) and D, 5 µM (56h, gray arrow).